PHYSICAL REVIEW B, VOLUME 64, 180510(R)

Electronic structures of antiperovskite superconductors $MgXNi_3$ (X=B, C, and N)

J. H. Shim, S. K. Kwon, and B. I. Min
Department of Physics, Pohang University of Science and Technology, Pohang 790-784, Korea
(Received 25 June 2001; published 19 October 2001)

We have investigated electronic structures of a newly discovered antiperovskite superconductor $MgCNi_3$ and related compounds $MgBNi_3$ and $MgNNi_3$. In $MgCNi_3$, a peak of very narrow and high density of states is located just below the Fermi level, which corresponds to the π^* antibonding state of Ni $3d$ and C $2p$ but with the predominant Ni $3d$ character. The prominent nesting feature is observed in the Γ-centered electron Fermi surface of an octahedron-cage-like shape that originates from the 19th band. The estimated superconducting parameters are in reasonable agreement with experiment, suggesting that the superconductivity in $MgCNi_3$ is described properly by the conventional BCS phonon mechanism.

DOI: 10.1103/PhysRevB.64.180510 PACS number(s): 74.25.Jb, 74.70.Ad, 71.20.−b

Recently, He *et al.*[1] have discovered a new intermetallic superconductor $MgCNi_3$ with the transition temperature of $T_c \sim 8$ K, which has the antiperovskite structure. Because it has a large proportion of Ni per unit cell, it is thought that the magnetic fluctuation would be important for its superconducting behavior. This system is reminiscent of another Ni-based superconductor, RNi_2B_2C (R=Y, Tm, Er, Ho, and Lu).[2–4] The band calculations indicate that a very large and narrow peak of mainly the Ni $3d$ character is located just below the Fermi energy E_F in the density of states (DOS) curve.[5,6] The behavior of the upper critical field $H_{c2}(T)$ can be well fitted with the conventional BCS expression,[7] whereas the zero-bias conductance peak observed below T_c has been interpreted as indicating a non-s-wave superconductor.[8]

With Cu doping (electron doping) on the Ni site, T_c decreases systematically, but with Co doping (hole doping), the superconductivity disappears abruptly for doping of only 1%.[5] In the case of Co doping, there is no evidence that the quenching of superconductivity is related to magnetism. Furthermore, it is observed that the superconductivity of MgC_xNi_3 is sensitive to the content of C; it disappears in between $x=0.96$–0.90.[1]

To understand the mechanism of the superconductivity in $MgCNi_3$, we have investigated systematically electronic structures of $MgXNi_3$ (X=B, C, and N), which have different numbers of valence electrons, but have similar band structures. Using the linearized muffin-tin orbital (LMTO) band method in the local density approximation (LDA), we have obtained band structures, DOS's, and Fermi surfaces, and discussed the bonding characters. Muffin-tin orbitals up to d states for Mg, C, and up to f states for Ni are included in the LMTO band calculations. We have also estimated superconducting parameters based on the rigid-ion approximation.

We have considered cubic $MgCNi_3$ with the lattice constant of $a=3.81$ Å (Ref. 1) and employed the atomic sphere radii of 3.20, 1.54, and 2.49 Å for Mg, C, and Ni, respectively. The same structural parameters are used for all $MgXNi_3$. $MgCNi_3$ has the cubic antiperovskite structure: Mg at (0 0 0), C at (0.5 0.5 0.5), and Ni at (0.5 0.5 0), (0.5 0 0.5), and (0 0.5 0.5). It is called as an antiperovskite structure because the transition metals are located at the corners of the octahedron cage in contrast to the ordinary perovskite structure.[9] Without C located at the center of cubic cell, $MgNi_3$ is a simple ordered intermetallic compound with the face-centered-cubic structure (Cu_3Au-type). Without C, the Ni $3d$ band in $MgNi_3$ is very narrow, leading to a magnetic ground state with Ni magnetic moment of $0.43\mu_B$.[10] By inserting C, two carbons become nearest neighbors of Ni, and thus it is expected that Ni $3d$ and C $2p$ electrons are strongly hybridized. Indeed, the LDA+U (U: Coulomb correlation parameter) band calculation for $MgCNi_3$ with $U=5$ eV yields essentially the same electronic structure as that of the LDA, indicating that the correlation effect of Ni $3d$ electrons is not so important.[10] It is because of their delocalized nature due to strong hybridization between Ni $3d$ and C $2p$ states.

The band structure of $MgCNi_3$ along the symmetry lines of the simple cubic Brillouin zone (BZ) is shown in Fig. 1. The band near -12 eV corresponds to C $2s$ states which is not shown in Fig. 1, while the dispersive bands between -7 eV and -4 eV are mostly due to C $2p$ states. Only two bands (the 18th and 19th bands), which have mainly Ni $3d$ character, cut the Fermi level. These two bands are confined between -0.5 eV and 1.0 eV, and the number of available states in these bands are about four. These bands are almost half-filled: only two electron states are occupied. Hence, in the rigid band scheme, small electron or hole doping will produce the conduction carriers with the 18th and the 19th band character. The 18th band is relatively flatter than the 19th band, and so the Ni $3d$ character is stronger in the 18th band.

The total and atomic site projected local DOS of $MgCNi_3$ are provided in Fig. 2. The overall shape of the total DOS is similar to those of Hayward *et al.*[5] and Dugdale and Jarlborg.[6] The peaks near -7 eV and 4 eV correspond to σ bonding and σ^* antibonding states, respectively, of Ni $3d$ and C $2p$ states. On the other hand, the peaks near -4 eV correspond to π bonding states of Ni $3d$ and C $2p$ electrons. The π^* antibonding states are located just below E_F, yielding the high DOS at E_F of $N(E_F)=5.34$ states/eV. The contribution of Ni $3d$ states to the DOS at E_F is as much as 76%. A small amount of C $2p$ states are mixed with Ni $3d$ states.

Because the peak located ~ 80 meV below E_F is very high and narrow, this system is expected to be unstable by

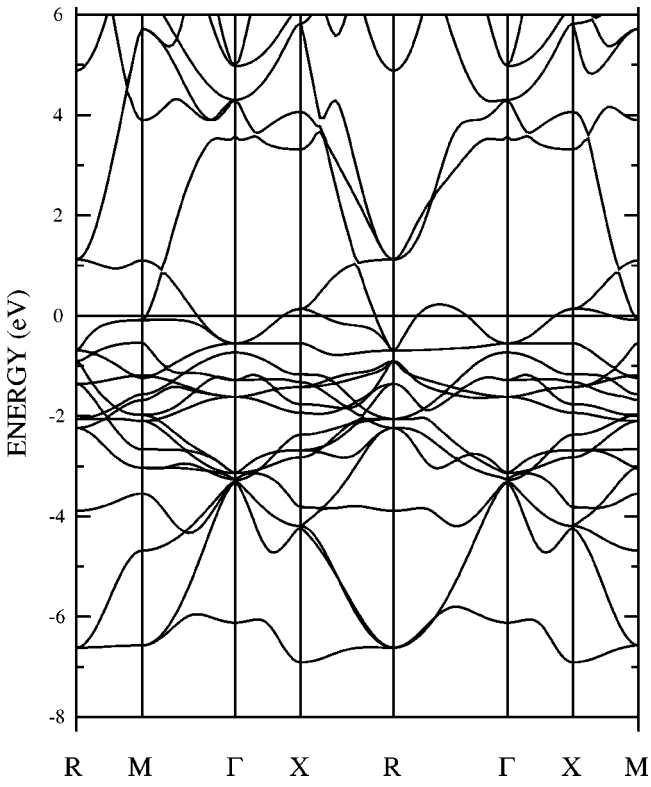

FIG. 1. Band structure of $MgCNi_3$ along the symmetry lines of the simple cubic BZ.

small hole doping. The Stoner exchange enhancement parameter S, defined as $S \equiv N(E_F) I_{XC}$ with I_{XC} denoting the intra-atomic exchange-correlation integral, is 0.64. Thus, small hole doping will induce the magnetic instability. Indeed the filling of holes in a rigid band scheme produces the magnetic instability. That is, replacing Ni by a virtual atom with atomic number 27.93 (corresponding to Co 7% doping) yields the Stoner parameter larger than 1.[10] This feature, however, is not consistent with the recent report that there is no evidence of long range magnetic ordering in the case of Co doping.[5] This point will be discussed further below.

Figure 3 presents the Fermi surfaces of the 18th and 19th bands and their changes by shifting the Fermi level on the ab plane ($k_z = 0$) in the BZ. The 18th band gives rise to a X-centered hole surface at each cubic face and small hole pockets along the [111] directions which are not shown in Fig. 3(a). With increasing the Fermi level (electron doping), the areas of these hole Fermi surfaces decrease, reducing $N(E_F)$. In contrast, with decreasing the Fermi level (hole doping), the Fermi surface areas increase, enhancing $N(E_F)$. When decreasing the Fermi level further below the DOS peak, the crossing of each hole surface occurs, converting it to Γ-centered circular electron surface on the ab plane and decreasing the Fermi surface. On the other hand, the 19th band yields an octahedron-cage-like electron surface centered at Γ which appears as square on the ab plane as shown in Fig. 3(b), and additional narrow electron surfaces along the BZ edges which appear as M-centered small pockets. With varying the Fermi level position, the 19th band shows a rather small change in the Fermi surface, as compared to the

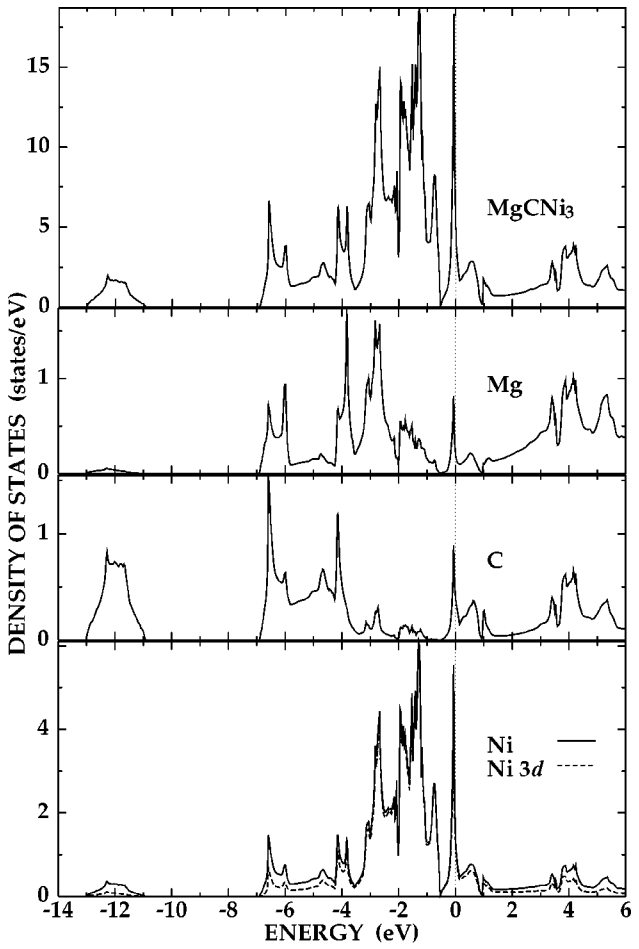

FIG. 2. The total and atomic site projected local DOS of $MgCNi_3$.

case of the 18th band. It is because of its more dispersive band character.

Most notable in Fig. 3(b) is the prominent nesting feature along the [110] direction in the Γ-centered Fermi surface with the square-like shape. Especially, with a 140 meV upward shift of E_F corresponding to the ~ 0.4 electron doping

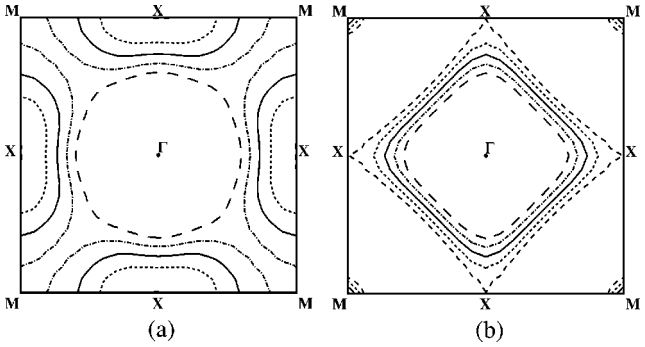

FIG. 3. The Fermi surface changes of the 18th (a) and the 19th band (b) by shifting the Fermi level on the $k_z = 0$ plane in the BZ. Each surface is drawn with the Fermi level shifts of $\Delta E_F = 140$ (dashed), 70 (dotted), 0, -70 (dot-dashed), and -140 meV (long-dashed) relative to the original E_F. The solid line represents the Fermi surface of the undoped case.

effect, the Fermi surface becomes exactly matching with zone boundary to show a perfect nesting feature.[11] In fact, this is contrary to the report by Dugdale and Jarlborg,[6] who have claimed that there is no obvious nesting feature in the Fermi surface of the 19th band. The detailed shapes of the Fermi surfaces are very sensitive to the position of the Fermi level, because of the very sharp DOS peak near E_F. Presumably the difference between these two results arises from the different band parameters employed in the LMTO band calculations, such as atomic radii, number of k points, energy parameters, and so on.[12] In any case, the present result reveals that the system is in the vicinity of the Fermi surface nesting, if not complete in undoped $MgCNi_3$.

It is well known that the system with the Fermi surface nesting can be strongly correlated with various instabilities: the structural transition (the charge density wave instability) or the spin density wave instability. It is thus expected that the electron doping of $MgCNi_3$ would be susceptible to one of the above instabilities. Based on this nesting feature, one could account for the experimental observation that the solubility of Cu is limited only up to $\sim 3\%$, while that of Co is much extensive.[5] Note, however, that any evidence of magnetic or structural transition has not been reported yet.[5,13] This aspect remains to be resolved. We have shown above that the hole doping in a rigid band scheme (virtual atom approximation) produces the magnetic instability, which seems to be contrary to the observation. Hence we have performed the supercell calculations for ordered $MgCNi_{3-x}Co_x$ ($x=0.25$, 0.5, and 1.0) assuming the same structural parameter as in $MgCNi_3$. Different from the case of the virtual atom approximation, the supercell calculations yield no magnetic instabilities,[10] in agreement with the experiment. This suggests that the simple rigid band scheme may not work well in the case of Ni site doping. Rather, Mg site doping will be better to reveal the perfect nesting feature, because the contribution of Mg states to the DOS at E_F is negligible as compared to those of Ni and C states.

To explore the doping effect with varying the number of valence electrons, we have investigated electronic structures of $MgXNi_3$ ($X=$B, C, and N). Figure 4 provides the DOS's for $MgXNi_3$. It is seen that the effect of changing X is mainly a variance of the Fermi level with respect to the DOS peak, even though the shape of DOS near E_F is perturbed a little bit.

The B $2p$ state in $MgBNi_3$ is located higher in energy than the C $2p$ state of $MgCNi_3$, and so the hybridization with Ni $3d$ is stronger. Hence the band is more dispersive and accordingly the DOS peak becomes smeared. Although the Fermi level in $MgBNi_3$ is located very close to the DOS peak, the DOS at E_F, $N(E_F)=4.79$ states/eV, is comparable to $N(E_F)=5.34$ states/eV of $MgCNi_3$ (Table I). Hence the magnetic instability does not occur either in $MgBNi_3$. As described before, the effective hole doping in $MgBNi_3$ converts the hole Fermi surface of the 18th band to an electron Fermi surface, and the electron surface of the 19th band is reduced smaller. In $MgNNi_3$, the N $2p$ state is located a bit lower in energy than the C $2p$ state of $MgCNi_3$, yielding reduced bandwidths of both the 18th and the 19th band. By the effective electron doping in $MgNNi_3$, the DOS at E_F is

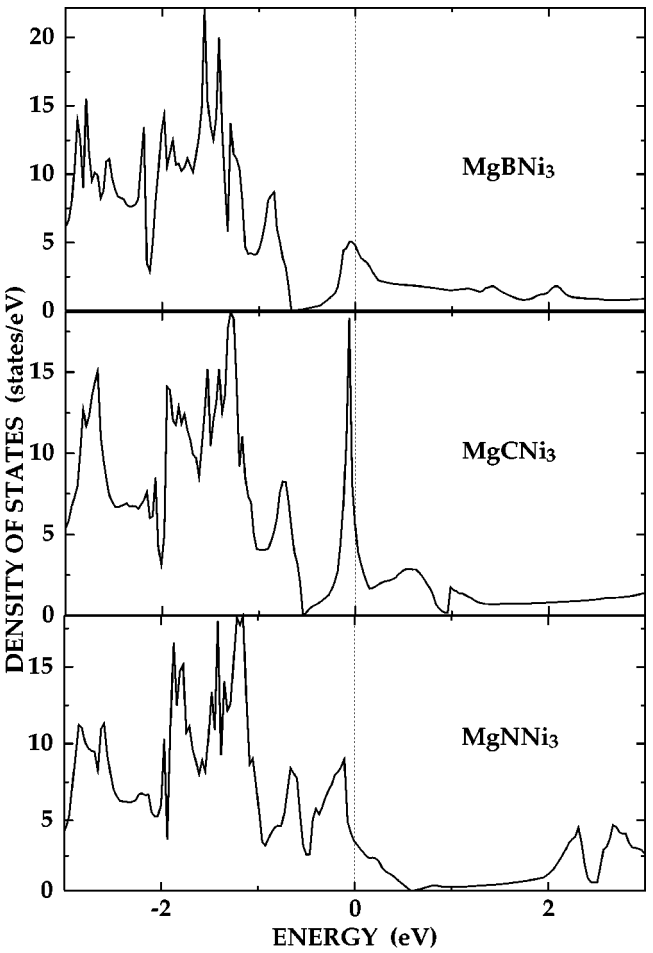

FIG. 4. Density of states of $MgXNi_3$ ($X=$B, C, and N).

reduced to 3.63 states/eV. The contribution of the 18th band to the DOS at E_F is almost negligible and the Fermi surface of the 19th band, which gives the main contribution to the DOS at E_F, is changed to a hole surface.

We have explored superconducting properties of $MgXNi_3$ based on the rigid-ion approximation.[14] We have estimated the superconducting parameter $\eta_\alpha = N(E_F)\langle I_\alpha^2\rangle$, where $\langle I_\alpha^2\rangle$ is the average electron-ion interaction matrix element for the αth ion. Table II provides the calculated η_α for each $MgXNi_3$. It is seen that the contribution of Ni $3d$ states to the superconductivity is most important and η_{Ni} is the largest for $MgCNi_3$. This is consistent with the observed trend that both the electron and hole dopings on $MgCNi_3$ suppress the superconductivity. By increasing the atomic number from B, C to N, the contribution of X $2p$ states η_X increases. Due to light ionic masses of X, even the small increase in η_X affects

TABLE I. The calculated total and partial DOS at E_F (in states/eV) for $MgXNi_3$ ($X=$B, C, and N).

	$N(E_F)_{Mg}$	$N(E_F)_X$	$N(E_F)_{Ni}$	$N(E_F)_{total}$
$MgBNi_3$	0.38	0.18	1.41	4.79
$MgCNi_3$	0.22	0.42	1.57	5.34
$MgNNi_3$	0.11	0.34	1.06	3.63

TABLE II. Comparison of η_α (eV/Å^2) and λ_{ph} for $\Theta_D = 300$ K and 400 K.

	η_{Mg}	η_X	η_{Ni}	λ_{ph} (300 K)	λ_{ph} (400 K)
$MgBNi_3$	0.00	0.22	0.67	0.67	0.38
$MgCNi_3$	0.00	0.48	1.36	1.36	0.77
$MgNNi_3$	0.00	0.58	0.87	1.07	0.60

the superconducting property substantially. Therefore, the effectively electron doped system $MgNNi_3$, once synthesized successfully in the antiperovskite structure, would have a comparable T_c to $MgCNi_3$.

One can evaluate the electron-phonon coupling constant λ_{ph} by using the McMillan's formula[15] $\lambda_{ph} = \Sigma_\alpha \eta_\alpha / M_\alpha \langle \omega_\alpha^2 \rangle$, where M_α is an ionic mass and $\langle \omega_\alpha^2 \rangle$ is the relevant phonon frequency. Since there has been no information on the relevant phonons, we instead use the average phonon frequency $\langle \omega^2 \rangle \simeq \Theta_D^2/2$, where Θ_D is the Debye temperature. However, even the value of Θ_D is not available. Albeit very crude, one can estimate Θ_D from the specific heat data:[1] ~ 300 K from the graph of C/T vs T^2. Using this information for $MgCNi_3$, one obtains $\lambda_{ph} = 1.36$, and then the McMillan's T_c formula with an effective electron-electron interaction parameter $\mu^* = 0.13$ gives rise to $T_c = 23$ K. These values seem to be too large, as compared to experimental T_c and the estimated $\lambda_{ph} \sim 0.8$ from the specific heat data.[1] Note, however, that λ_{ph} strongly depends on the choice of the Debye temperature. As shown in Table II, with a choice of larger $\Theta_D = 400$ K, one obtains $\lambda_{ph} = 0.77$ and $T_c = 11$ K, which are in reasonable agreement with experiment. Moreover, in view of the rather large Stoner parameter in $MgCNi_3$, one may have to take into account the spin-fluctuation effect on the superconducting property. One can use the modified T_c formula including the spin-fluctuation parameter μ_{sp} in the McMillan's form.[16] Indeed, when considering small $\mu_{sp} = 0.1$, we have obtained much reduced $T_c = 11.5$ K even in the case of $\Theta_D = 300$ K. These estimations suggest that the superconductivity in this system can be described properly by the conventional phonon mechanism. However, for more precise estimations of λ_{ph} and T_c, detailed information on the phonon spectra is required.

In conclusion, we have investigated electronic structures of the nonoxide antiperovskite superconductor $MgCNi_3$. The π^* antibonding state of Ni $3d$ and C $2p$ is formed near E_F with the mainly Ni $3d$ character. The Fermi surfaces are composed of two bands. The topology of hole Fermi surfaces coming from the 18th band is sensitively modified by the variance of the Fermi level position. The electron surface of the 19th band with an octahedron-cage shape tends to induce the Fermi surface nesting. By comparison of the DOS's for $MgXNi_3$ (X = B, C, and N), the doping effects are discussed. The estimation of λ_{ph} and T_c based on the rigid-ion approximation suggests that the superconductivity of $MgCNi_3$ is described well by the conventional BCS phonon mechanism.

This work was supported by the KOSEF through the eSSC at POSTECH and in part by the BK21 Project. Helpful discussions with N.H. Hur are greatly appreciated.

[1] T. He *et al.*, Nature (London) **411**, 54 (2001).
[2] R. Nagarajan *et al.*, Phys. Rev. Lett. **72**, 274 (1994).
[3] R.J. Cava *et al.*, Nature (London) **367**, 252 (1994).
[4] W.E. Pickett and D.J. Singh, Phys. Rev. Lett. **72**, 3702 (1994); L.F. Mattheiss, Phys. Rev. B **49**, 13 279 (1994); J.I. Lee *et al.*, *ibid.* **50**, 4030 (1994).
[5] M.A. Hayward *et al.*, Solid State Commun. **119**, 491 (2001).
[6] S.B. Dugdale and T. Jarlborg, Phys. Rev. B **64**, 100508 (2001).
[7] S. Y. Li *et al.*, Phys. Rev. B **63**, 132505 (2001).
[8] Z.Q. Mao *et al.*, cond-mat/0105280 (unpublished).
[9] D.A. Papaconstantopoulos and W.E. Pickett, Phys. Rev. B **45**, 4008 (1992); P.R. Vansant, P.E. Van Camp, V.E. Van Doren, and J.L. Martins, *ibid.* **57**, 7615 (1998); A.L. Ivanovskii, R.F. Sabiryanov, and A.N. Skazkin, Fiz. Tverd. Tela (St. Petersburg) **40**, 1667 (1998) [Phys. Solid State **40**, 1516 (1998)]; W.S. Kim, E.O. Chi, J.C. Kim, H.S. Choi, and N.H. Hur (private communication).
[10] J.H. Shim, S.K. Kwon, and B.I. Min (unpublished).
[11] If the nesting feature exists only on the ab plane connecting the Fermi surface lines, the effect would be minor. We, however, have observed that there occurs a nesting feature with electron doping also on the (110) plane along the [110].
[12] The effect of atomic radii is rather large, and so we have chosen the optimized ones which yield a result similar to the full potential linearized augmented plane wave calculation of Ref. 5.
[13] Q. Huang *et al.*, cond-mat/0105240 (unpublished).
[14] G.D. Gaspari and B.L. Gyorffy, Phys. Rev. Lett. **28**, 801 (1972).
[15] W.L. McMillan, Phys. Rev. **167**, 331 (1967).
[16] T. Jarlborg and A.J. Freeman, Phys. Rev. B **22**, 2332 (1980); S.V. Vonsovski, Yu. A. Izyumov, and E.Z. Kurmaev, *Superconductivity of Transition Metals*, Springer Series in Solid State Sciences Vol. 27 (Springer-Verlag, Berlin, 1982).